Breakthrough in a flat channel membrane microcontactor

Reference:

Hereijgers Jonas, Breugelmans Tom, De Malsche Wim.- *Breakthrough in a flat channel membrane microcontactor*

Chemical engineering research and design - ISSN 0263-8762 - (2014), p. 1-22

DOI: http://dx.doi.org/doi:10.1016/j.cherd.2014.12.004

Breakthrough in a flat channel membrane microcontactor

Jonas Hereijgers[a,b], Tom Breugelmans[b,c] and Wim De Malsche[a*]

[a]*μFlow, Department of Chemical Engineering, Vrije Universiteit Brussel, Pleinlaan 2, 1050 Brussel, Belgium*
[b]*Faculty of Applied Engineering, Research group Advanced Reactor Technology, University of Antwerp, Salesianenlaan 90, 2660 Hoboken, Belgium*
[c]*Research Group Electrochemical and Surface Engineering, Vrije Universiteit Brussel, Pleinlaan 2, 1050 Brussel, Belgium*

Email: jhereijg@vub.ac.be, tom.breugelmans@uantwerpen.be, wdemalsc@vub.ac.be

*Corresponding author: tel. (+) 32/ 2.629.33.18, fax (+) 32/ 2.629.32.48, e-mail:

wdemalsc@vub.ac.be

Abstract

In literature three different models describing the breakthrough pressure were identified: the Young-Laplace model, the Kim-Hairrott-Zha model and the Franken et al. model. However, large differences between experimental results and model are often reported and a comparative study is lacking. In the present study, the different models were experimentally validated by measuring breakthrough pressures in liquid/liquid systems. The average differences between model and experimental results for the three models were respectively 37.5 %, 26.7 % and 32.2 %. The Kim-Harriott-Zha model obtained the best results, however for the model it is advised that a solvent system with a low contact angle is searched to determine the maximum correction angle. Therefore a fourth model was proposed omitting this step and yielding an average deviation of 25.0 %.

Keywords

breakthrough pressure; critical entry pressure; membrane contactor; liquid-liquid extraction; parallel flow

1. Introduction

Membrane contactors are interesting tools in separation processes, which have evolved the last two decades into well accepted unit operations (Pabby and Sastre, 2013). The membrane immobilizes the interface between two phases, liquid-liquid or gas-liquid, thereby allowing operation in parallel flow without mixing or disrupting the flows. In this way liquid-liquid extraction can for instance be performed, hence omitting a compulsory often slow phase separation step. A disadvantage of classical liquid-liquid extraction is indeed the formation of stable emulsions, but also foaming, unloading and flooding often poses problems (Gabelman and Hwang, 1999). Combining a membrane with shallow channels, high mass transfer kinetics can be easily reached (Hereijgers et al., 2013), requiring only a few minutes to obtain thermodynamic equilibrium. Kiani et al. (1984) and D'Ella et

al. (1986) demonstrated this in different membrane configurations, using both a flat membrane and hollow fibers. Several applications have been reported, such as the removal of phenols out aqueous waste streams (González-Muñoz et al., 2003). Using 1-decanol as solvent and a concentrated aqueous NaOH solution as stripping solvent in a second membrane contactor, 99 % of the phenol could be removed. Bocquet et al. (2006) extracted aroma compounds from aqueous solvents using n-hexane and Dupuy et al. (2011a) extracted terpenes from lemon essential oil. For the recovery of metal ions Maruyama et al. (2004) built a microfluidic channel with intermittent partition walls instead of a membrane to pin the interface between the pillars, creating a stabilizing effect.

Supported liquid membrane (SLM) extraction is a special case of membrane extraction (Audunsson, 1986, Jönsson et al., 1993). In SLM the pores are filled with a wetting organic solvent and the channels at both sides of the membrane contain water-based solvents at a different pH. Chargeable solutes enter the contactor at a pH value at which they are uncharged, enabling transport through the organic solvent. Once entered in the aqueous acceptor phase, the solutes become charged due to a different pH, preventing them from back-diffusion. SLM is a technique primarily used in sample preparation, where the acceptor phase often stands still, pre-concentrating the sample prior to analysis. Additionally an electric field can be applied across the membrane to accelerate mass transfer. Pedersen-Bjergaard and Rasmussen (2006) demonstrated this, by immersing a polypropylene hollow fiber housing the acceptor solution and holding the organic solvent (typically 2-nitrophenyl octyl ether) in the pores into the donor solution. The hollow fiber was mechanically closed at one end preventing leakage of the acceptor solution into the donor solution. Placing an electrode in each phase a recovery of 70 to 80 % was reached in typically 5 min only, extracting various basic drug substances such as pethidine, nortriptyline, methadone, haloperidol and loperamide.

Besides liquid-liquid extraction, membranes are also used as interface stabilizer in membrane distillation modules or gas absorption modules. Using a hydrophobic membrane, the aqueous liquid feed is fixed at the pore mouths, preventing it from entering or wetting the pores. Only vapor is

hence able to migrate through the pores. A cold aqueous liquid or surface at the other side of the membrane can subsequently condense the vapor inside the module. Alternatively a sweeping gas or vacuum can be used requiring however a large external condenser (Alkhudhiri et al., 2012).

Membrane distillation is applied for several applications such as desalination (Banat and Simandl, 1998), removal of heavy metals (Zolotarev et al., 1994) and treatment of organic polluted aqueous waste streams (El-Abbassi et al., 2011). For gas absorption one side of the membrane is contacted with liquid and the other side with gas. Mavroudi et al. (2006) examined in this way the mass transfer resistance of CO_2 absorption using a hollow fiber.

Critical in all these membrane operations is the stability of the parallel flow profile, which is the purpose of the membrane. By capillary action the interface between both phases should be pinned preferably at the pore mouth. If the interface is pinned inside the pores, the membrane is partially wetted, and has as a consequence a negative impact on the mass transfer in gas-liquid absorption. Wang et al. (2005) reported a reduction of as much as 20 % of the global mass transfer coefficient even if the pores are only 5 % wetted. When the operation conditions are not carefully selected, the pressure difference across the membrane can become excessive. At that moment one of the phases will flow through the pores and disperse in the other phase, making phase separation again necessary and the membrane irrelevant. This phenomenon is called breakthrough. However, the operation conditions or pressure difference across the membrane at which this occurs are often differently defined in the literature and no comparative study is performed.

In the present paper, the validity of different models describing the breakthrough pressure is examined by experimentally measuring breakthrough pressures, focusing on liquid-liquid extraction systems.

2. Breakthrough pressure models

Based on the pressure profile of both phases two situations can be defined. In the first situation the pressure of the non-wetting phase is higher than the pressure of the wetting phase. In this classical situation the non-wetting phase will not enter the pores by capillary forces, holding the interface at the pore mouth. At the breakthrough pressure, also called the critical entry pressure, the non-wetting phase will penetrate through the pores and disperse in the wetting phase. To calculate this breakthrough pressure the Young-Laplace law (Eq. 1) is most often used in the literature (Alkhudhiri et al., 2012, García-Payo et al., 2000, Bougie and Illiuta, 2013, Saffarini et al., 2013, Dupuy et al., 2011b, Lawson and Lloyd, 1997):

$$\Delta P_b = \frac{-2\gamma\beta cos\theta}{r} \quad (1)$$

with γ the interfacial tension between the two immiscible liquids in liquid-liquid operation. In gas-liquid operations γ is replaced by the surface tension σ. The influence of the pore shape is represented by β. The Young-Laplace law is defined for cylindrical pores and therefore β is often lacking, as a value of 1 is assumed in that case. For irregular shapes a value between 0 and 1 is found. θ is the contact angle between liquid 1, liquid 2 or gas phase and the membrane material and r is the maximum pore radius.

Instead of correcting the Young-Laplace equation using the β-coefficient, Kim and Harriott (1987) proposed a different model (Eq. 2). They noticed that some membranes have a fibrous structure like paper or a mat of glass wool and that the pores are the irregular spaces between the adjacent fibers. Therefore Kim and Harriott (1987) assumed it is more accurate to describe the pores as a donut-like geometry, resulting in the following model (Eq. 2) to describe the breakthrough pressure.

$$\Delta P_b = -\frac{2\gamma\cos(\theta-\alpha)}{r\left(1+\frac{R}{r}(1-\cos\alpha)\right)} \quad (2)$$

with γ the interfacial or surface tension, θ the contact angle, r the smallest pore radius along the pore passage holding the largest pore bottleneck, R the radius of the fibers of the membrane forming the pores (Fig.2) and α the correction angle for the pore shape which can be calculated from the contact angle. Setting the derivative of (Eq. 2) to zero yields the following equation (Eq. 4), from which α can be calculated:

$$\frac{d(\Delta P_b)}{d\alpha} = 0 \quad (3)$$

$$\sin(\theta-\alpha) = \frac{\frac{R}{r}\sin\theta}{1+\frac{R}{r}} \quad (4)$$

For air-liquid systems the model yields adequate correlations but for liquid-liquid system deviations are large and unsatisfactory (Kim and Harriott, 1987), unfortunately no explanation for these observations is given. Zha et al. (1992) proposed a similar model as (Eq. 2) by studying SLM systems and introduced a restriction for the correction angle α. Its absolute value can never be higher than the maximum correction angle α_m. An estimate of α_m is obtained by measuring the breakthrough pressure with a solvent system with a low contact angle. Zha et al. (1992) used a 25 % aqueous ethanol solution and air as the second phase to measure this and proceeded as follows. r and R/r are estimated from nonlinear regression using (Eq. 2) by measuring the breakthrough pressure and the contact angle for a range of different solvent systems. Knowing this, α_m is estimated from (Eq. 2) using the breakthrough pressure for the 25 % aqueous ethanol/air system. If the absolute value of the correction angle from (Eq. 4) is larger than α_m, α_m should be used in (Eq. 2) to calculate the breakthrough pressure. Zha et al. (1992) tested this model for three different membranes: Durapore HVHP ($d_{pore,\,max,\,manufacturer}$ = 1.6 µm, $d_{pore,\,max,\,fit}$ = 1.30 µm), Celgard 2500 ($d_{pore,\,max,\,manufacturer}$ = not given, $d_{pore,\,max,\,fit}$ = 0.34 µm) and Accurel 2E-PP ($d_{pore,\,max,\,manufacturer}$ = 0.81 µm, $d_{pore,\,max,\,fit}$ = 0.80 µm) and

concluded that the fitted maximal pore sizes were in agreement with those provided by the manufacturers. Zha et al. (1992) also pointed out that r and R can be estimated from SEM pictures of the membrane. Caution should however be taken as the pore shape is often irregular making it difficult to correctly estimate the pore size from a SEM picture.

Franken et al. (1988) also studied the model of Kim and Harriott (1987) and proposed that this model is only valid when the pore edges are "rounded". However, when the pores of the membrane are "sharp-edged" the denominator of (Eq. 2), which can be seen as a hydraulic radius, has to be modified (Eq. 5):

$$\Delta P = -\frac{2\,\gamma\,cos\,(\theta - \alpha)}{R\,cos\alpha} \tag{5}$$

The breakthrough pressure is reached when the meniscus has to overcome the narrowest point in the pore. This 'sharp-edged' barrier is overcome when ΔP equals (Eq. 6):

$$\Delta P_b = -\frac{2\,\gamma\,cos\,(\theta + \alpha_m)}{r} \tag{6}$$

At the sharp-edged barrier, $R\cos\alpha$ equals r as the pore is then at its narrowest point. However, as indicated by Franken et al. (1988) most of the membranes have rounded pores and the sharp-edged structure is only obtained with special production processes (e.g. thermal inversion with slow cooling).

From all the models it is clear that the interfacial tension, the contact angle and the pore radius and morphology are the deciding factors that determine the breakthrough pressure. However, it is not clear which model is most suitable to predict the breakthrough pressure under common conditions. In the first situation the pressure of the non-wetting phase was higher than that of the wetting phase. In the second situation the pressure of the wetting phase is higher than that of the non-wetting phase. This is always an undesirable state as breakthrough will always occur. This is logical since there is no capillary action anymore holding back the liquid.

3. Material and Methods

3.1 Chemicals

The water used throughout the experiments was prepared in the laboratory (Milli-Q-gradient, Millipore, Bedford, MA, USA). Methyl isobutyl keton (MIBK) was purchased from Acros Organics and the remaining chemicals used were purchased from Sigma-Aldrich. All chemicals were of analytical reagent grade.

3.2 Breakthrough pressure

The breakthrough pressure was determined for 5 different water/organic solvent systems (n-heptane, 1-octanol, ethyl acetate, MIBK and toluene) and two different flat sheet membranes (Table 1).

Table 1: Specifications of the examined membranes provided by the manufacturer.

Material	Manufacturer	Porosity (%)	Thickness (µm)	Pore Size (nm)
PTFE	Frisenette Aps	68.0	70	100[a]
Polypropylene	Celgard	55	25	64[b]

a: Measured by the bubble point test method

b: Measured by the water intrusion test method

The membrane was clamped between two aluminum bodies with a channel of 13 mm wide, 90 mm long and 100 µm deep. Pillars of 1 mm in an equilateral triangle pattern with a spacing of 2 mm were defined inside the channel to support the membrane, resulting in a membrane area of 12 cm² (Hereijgers et al., 2012, 2013). Rinsing with methanol was first performed in both channels at a flow rate of 5 mL/min with an HPLC pump (Shimadzu) to remove all the air. Using syringe pumps (kd

Scientific) water and the organic solvent were fed into the membrane microcontactor (MMC) at a flow rate of 50 µL/min (Fig. 1a). Using a backpressure regulation valve at the outlet of the MMC, the pressure at the non-wetting side of the membrane was gradually increased until breakthrough was observed. The pressures at both inlets and outlets were monitored using 4 pressure transducers (Gefran, model no. TK-N-1-E-B01D-H-V). Once breakthrough was observed the pressure difference at that moment across the membrane revealed the critical pressure. Every breakthrough pressure was measured three times. In order to check if the design of the MMC or the flow of the liquids has an influence on the breakthrough pressure, the breakthrough pressure for the 5 solvent systems was also measured for the PTFE membrane using a sample holder and a pressurized vessel (Fig. 1b). A pre-cut piece of the PTFE membrane (72 mm²) was clamped between two aluminum bodies. The organic wetting solvent was applied on top and water the non-wetting solvent was allowed to flow for a few minutes underneath the membrane to remove all the air bubbles. Once all the air was removed this exit was closed and the pressure was gradually increased using a pressure regulator until breakthrough was visually observed. This was repeated three times.

The different models and set-ups were compared by calculating the average difference between the measured breakthrough pressure and the one predicted by the model as follows (Eq. 7).

$$\varepsilon = \frac{100\%}{n} \sum_{j=1}^{n} \frac{|\Delta P_{b,j,m} - \Delta P_{b,j,c}|}{\Delta P_{b,j,m}} \quad (7)$$

with ε the average difference and n the number of measurements.

Fig. 1: Schematic drawing of the set-ups to measure the breakthrough pressure. a) MMC set-up: ❶ syringe pump, ❷ pressure transducer, ❸ MMC, ❹ backpressure regulation valve b) Sample holder set-up: ❶ nitrogen gas bottle, ❷ pressure controller, ❸ pressurized vessel, ❹ sample holder.

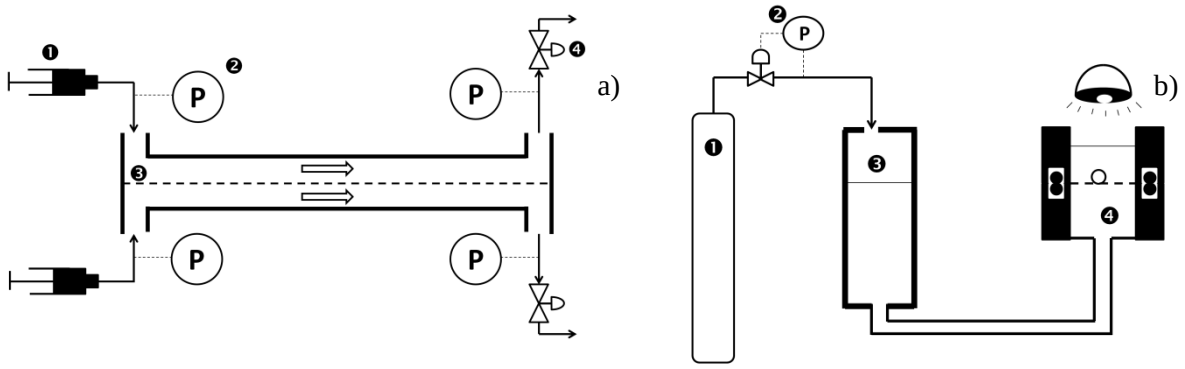

3.3 Contact angle

The contact angles were measured with the sessile drop method (KrüssKR DSA30). A piece of the membrane was clamped and submerged in the wetting liquid in a cuvette and a 5 µL droplet of the non-wetting liquid was dispensed, using an automated syringe of 10 µL. Once the droplet rested onto the membrane a picture was taken sideways from which the contact angle was determined.

4. Results

4.1 Study of the breakthrough models

The contact angle and breakthrough pressures were first measured for different solvents for the PTFE and PP membranes (see table 2). The interfacial tension value was taken from literature (North, 1999). The breakthrough pressure of n-heptane and toluene could not be determined for the polypropylene membrane, because the pressure to be measured lied above the maximum operating pressure of 10 bar of the used pressure transducers. These results were used to calculate the breakthrough pressures ($\Delta P_{b,c}$) for the different models in order to check their validity. The free parameters of each model were fitted by the sum of least squared values.

Table 2: Contact angle and breakthrough pressure results measured using the MMC set-up (Fig. 1a).

		PTFE membrane		PP membrane	
	γ (mN/m)[a]	$\Delta P_{b,m}$ (bar)	θ (°)	$\Delta P_{b,m}$ (bar)	θ (°)
n-Heptane	51	3.03 ± 0.14	128.4 ± 2.5	OR[b]	/
1-Octanol	8.52	0.59 ± 0.12	133.6 ± 3.5	4.17 ± 0.09	123.8 ± 5.1
MIBK	15.7	0.74 ± 0.01	138.6 ± 4.2	4.24 ± 0.28	105.9 ± 5.6
Ethyl Acetate	6.79	0.52 ± 0.02	133.5 ± 1.5	1.19 ± 0.05	127.9 ± 4.0
Toluene	36.1	2.58 ± 0.07	123.1 ± 2.9	OR[b]	/

a: North (1999)

b: Out of detection range (> 10bar)

The first examined model was the Young-Laplace model (Fig. 3a) (Eq. 1). β was obtained by fitting for the PTFE and PP membrane, resulting respectively in values of 0.51 and 2.36. As β should theoretically lie between 0 and 1, this was clearly not the case for the PP membrane. A possible explanation is that the given pore size by the manufacturer was underestimated. For the Young-Laplace model, the average difference between the calculated and measured breakthrough pressure was 37.5 %. The second model (Eq. 2) that was evaluated was the one described by Kim-Harriott (1987) and Zha et al. (1992) (Fig. 3b). As stated by Zha et al. (1992), α_m is best determined with a solvent system where the contact angle is low (referred to as advancing contact angle in Zha et al., (1992)), as the importance of α increases with a decreasing contact angle. Zha et al. (1992) used an air-25 % ethanol mixture with contact angles equal or below 100 °. As for the PTFE membrane, all the contact angles were more than 20 ° higher it can be assumed that α_m was not reached. Nonetheless with toluene-water giving the smallest contact angle, its α_m equaled to -56.9 ° which is in absolute terms larger than all the α obtained for the other solvent systems justifying the made assumption. For the PP membrane α_m equaled to -27.7 ° determined out of the MIBK-water system. r and R/r determined by the best fit with R/r restricted to be non-negative for the PTFE membrane were

respectively 319 nm and 0.0 and for the PP membrane 43 nm and 1.7 and the average deviation equaled 26.7 %. The Kim-Harriott-Zha model resulted in a better relation than the Young-Laplace model, which is not completely surprising as two fitting parameters instead of one were used. The best fit R/r value for the PTFE membrane was zero. When looking at the SEM picture of the membrane (Fig. 2a) R/r should indeed be very small as the membrane consists of very thin overlapping and cross-linked fibers. For the PP membrane (Fig 2b) it was more difficult to see if the R/r value corresponds to the observed geometry as there is a large spread in R.

Fig. 2: SEM pictures of the PTFE membrane (a) and PP membrane (b). An example of R (Eq. 2) is given in (a).

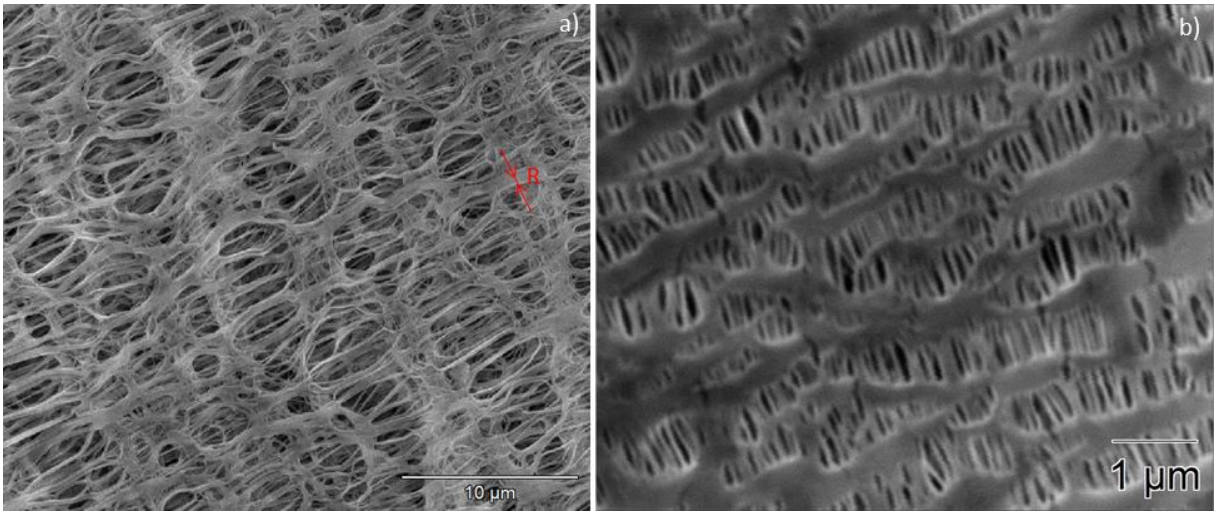

The third model evaluated was that described by Franken et al. (1988) (Fig. 3c) (Eq. 6). Just as the two previous models the fitting parameter in this case α_m was determined by a best fit, which was equal to 124.1 ° and 48.8 ° for the PTFE and PP membrane respectively. The average deviation was equal to 32.2 %. As this model is only valid when the pores have sharp edges which are not common (Franken et al., 1988), it is not surprising that it results in a fit of poorer quality. Observing the SEM pictures of the two tested membranes (Fig. 2) it was clear that the pores are indeed rounded and not sharp-edged.

From the three models the Kim-Harriot-Zha model turned out to give the best fit, using two fitting parameters only. Looking at the Young-Laplace and the Franken model, one could state that the

241 fitting parameters compensate for the pore shape. Combining both parameters a fourth model (Eq.
242 8) could be composed:

$$\Delta P_b = -\frac{2\gamma\beta cos(\theta + \alpha)}{r} \quad (8)$$

243 Using both an α- and β-parameter an average deviation of 25.0 % was obtained (Fig. 3d). This is an
244 improvement of around 10 % compared to the Young-Laplace and Franken model, and a slight
245 improvement compared to the Kim-Harriot-Zha model, but which requires a system with a low
246 contact angle to determine α_m. β was 0.5 and 1.2 for the PTFE and PP-membrane respectively and α
247 was 105.9 ° and 30.1 °.
248
249 **Fig. 3: The measured breakthrough pressure vs. the calculated breakthrough pressure with the respective models:**
250 **a) Model of Young-Laplace, b) Model of Kim-Harriott-Zha, c) Model of Franken et al., d) Fourth model combining α**
251 **and β (Eq. 8) (× PTFE, ◇ PP). The solid line corresponds to the values expected according to the model.**

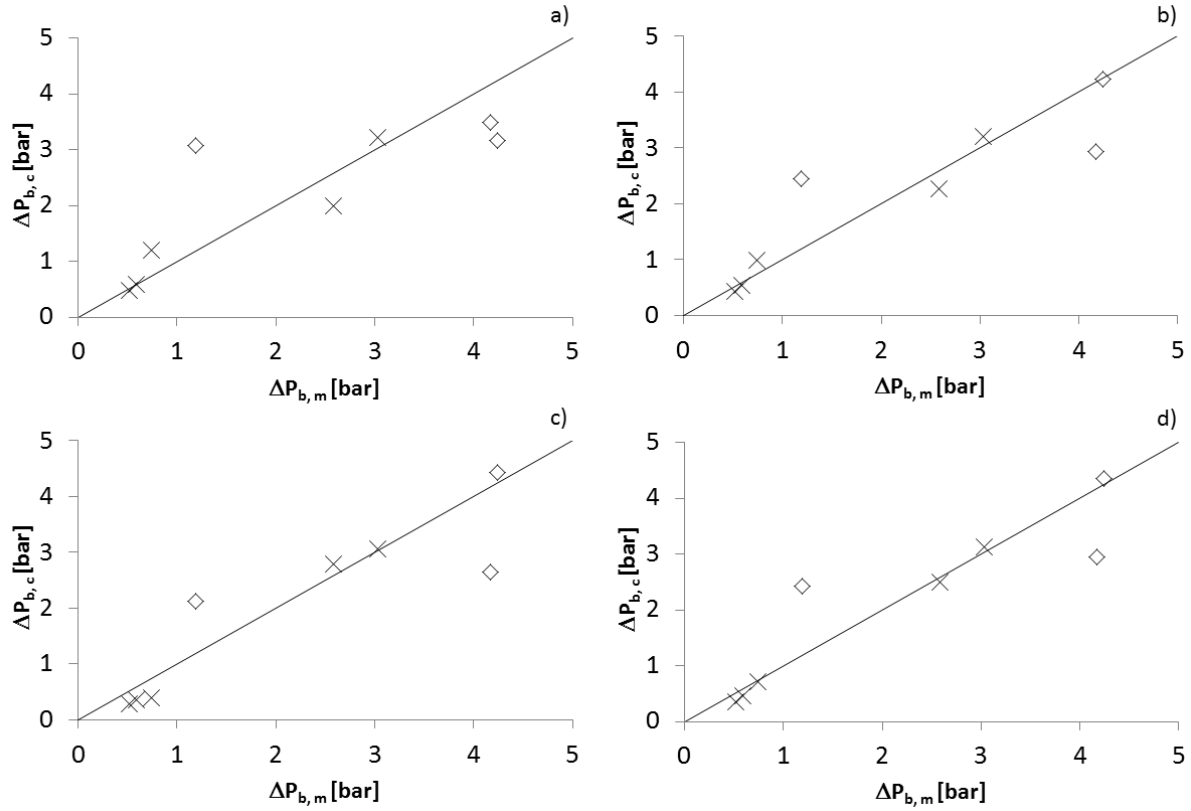

252
253

4.2 Influence of operating conditions

In order to verify whether it was correct to measure the breakthrough pressure with the MMC module the breakthrough pressure was also measured using a second set-up (Fig. 1b, Table 3). Using a pressure vessel the pressure can be increased until breakthrough is observed in such a way that there was no movement of the liquids. Besides the normal pressure difference across the membrane during flow, there is also a tangential stress exerted by the friction of the flowing fluids (Berthier et al., 2009). This raised the question whether it influences the breakthrough pressure, however as reported by Berthier et al. (2009) it is expected to be negligible.

The breakthrough pressures of both set-ups are depicted in Fig. 4 with an average difference of 2.4 % between the two methods. It is thus possible to predict the breakthrough pressure in future MMC experiments by measuring the breakthrough pressures of a few solvent systems using the same MMC set-up and there is hence no need for building a second set-up.

Table 3: Breakthrough pressure results measured using the sample holder set-up.

	n-Heptane	1-Octanol	MIBK	Ethyl Acetate	Toluene
$\Delta P_{b,m}$ (bar)	3.25 ± 0.10	0.52 ± 0.02	0.68 ± 0.01	0.33 ± 0.04	2.27 ± 0.04

Fig. 4: The measured breakthrough pressures vs. the calculated breakthrough pressure according to the modified Young-Laplace model (Eq. 8) for the PTFE membrane using the MMC set-up (×) and the sample holder set-up (◇).

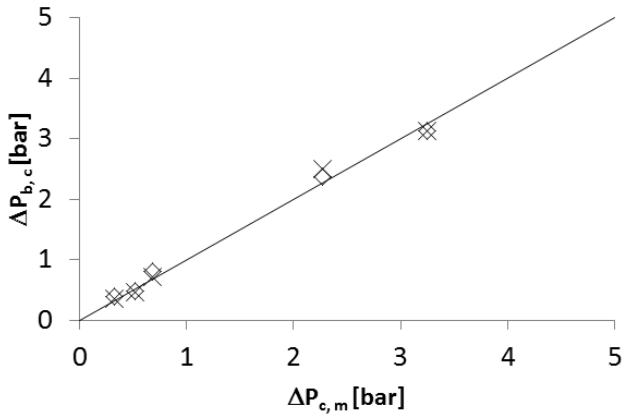

Comparing the four models the preference is given to the fourth proposed model (Eq. 8) as it gives the best correlation and no special solvent system is required to obtain the fitting parameters as well. Once they are known it is only necessary to measure the contact angle to have a reasonable estimation of the breakthrough pressure, this is important when one wants to operate the system for a longer period of time (Prasad and Sirkar, 1990). By continuously monitoring the trans-membrane pressure, process parameters such as back pressure or flow rates can be regulated, ensuring a stable operation.

It was observed from the SEM pictures (Fig. 2) that both membranes have a large pore size distribution which cannot be neglected. Knowing that the maximum pore size has a big influence on the breakthrough pressure, further improvement is possible here. Van Rijn (2004) produced such a membrane for microfiltration using an etching step after laser interference or deep UV lithographic definition of the pores. Fully cylindrical pores with pore sizes as small as 100 nm and thicknesses beneath 1µm were demonstrated. For this membrane, the Laplace model can be used, due to the cylindrical and smooth pore shapes. Using supporting beams, the maximum allowed transmembrane pressure upon rupture was estimated to be 2 bar, which allows for high liquid velocities. Even though the kinetics of extraction is reduced by the relatively low overall porosity (25%, Van Rijn (2004)) of the membrane, due to the presence of these support beams and the thickness of the walls in between the pores (in order to guarantee mechanical stability), the potential of this membrane format cannot be underestimated. The membrane thickness of 1 µm yields a negligible mass transfer resistance and with state-of-the art micromachining techniques wafer sizes of 30 cm diameter can be achieved. The high cost will however probably prevent a widespread implementation on the short term. Also taking fouling into consideration, which becomes of greater importance at reducing pore sizes, it can be expected that the average user will stick to disordered membranes, which can be easily produced with maximal pore sizes with sub-micron dimensions, for which the models studied in this paper are of high significance.

5. Conclusions

Three different models from the literature describing the breakthrough pressure were compared using experimentally measured breakthrough pressures for a set of liquid/liquid combinations and two different membranes (PTFE and PP). The Young-Laplace and the Franken et al. model gave an average deviation of 37.5 % and 32.2 % while the Kim-Harriott-Zha model produced an average deviation of 26.7 %. A disadvantage of this latter model is that a search for a solvent system with low contact angle is advised to find α_m. For this reason, the fitting parameters α and β from the Young-Laplace and Franken et al. model were combined into a fourth model to take the pore shape better into account, on the one hand yielding a slightly better fit of 25.0 %, but more importantly on the other hand avoiding a search of α_m.

6. Acknowledgements

W. De Malsche greatly acknowledges the Flemish Fund for Scientific Research (FWO) for support through a Post-Doctoral grant. J. Hereijgers is supported through a specialization grant from the Instituut voor Wetenschap en Technologie (IWT) from the Flanders region.

7. References

Alkhudhiri, A., Darwish, N., Hilal, N., Membrane distillation: A comprehensive review, Desalination 287 (2012), 2-18, DOI: 10.1016/j.desal.2011.08.027.

Audunsson, G., Aqueous/Aqueous Extraction by Means of a Liquid Membrane for Sample Cleanup and Preconcentration of Amines in a Flow System, Analytical Chemistry 58 (1986, 2714-2723, DOI: 10.1021/ac00126a030.

Banat, F.A., Simandl, J., Desalination by membrane distillation: a parametric study, Sep. Sci. Technol. 33 (2) (1998), 210-226, DOI: 10.1080/01496399808544764.

Berthier, J., Van-Man Tran, Mittler, F., Sarrut, N., The physics of a coflow micro-extractor: Interface stability and optimal extraction length, Sensors and Actuators A 149 (2009), 54-64, DOI: 10.1016/j.sna.2008.10.005.

Bocquet, S., Gascons Viladomat, F., Muvdi Nova, C., Sanchez, J., Athes, V., Souchon, I., Membrane-based solvent extraction of aroma compounds: Choiche of configurations of hollow fiber modules based on experiments and simulation, Journal of Membrane Science 281 (2006), 358-368, DOI: 10.1016/j.memsci.2006.04.005.

Bougie, F., Illiuta, M.C., Analysis of Laplace-Young equation parameters and their influence on efficient CO_2 capture in membrane contactors, Separation and Purification Technology 118 (2013), 806-815, DOI: 10.1016/j.seppur.2013.08.035.

D'Ella, N.A., Dahuron, L., Cussler, E.L., Liquid-liquid extractions with micro-porous hollow fibers, Journal of Membrane Science 29 (1986), 309-319, DOI: 10.1016/S0376-7388(00)81269-7.

Dupuy, A., Athes, V., Schenk, J., Jenelten, U., Souchon, I., Solvent extraction of highly valuable oxygenated terpenes from lemon essential oil using a polypropylene membrane contactor: potential and limitations, Flavour and Fragrance Journal 26 (2011a), 192-203, DOI: 10.1002/ffj.2052.

Dupuy, A., Athes, V., Schenk, J., Jenelten, U., Souchon, I., Experimental and theoretical considerations on breakthrough pressure in membrane-based solvent extraction: Focus on citrus essential oil/hydro-alcoholic solvent systems with low interfacial tension, Journal of Membrane Science 378 (2011b), 203-213, DOI: 10.1016/j.memsci.2011.05.005.

El-Abbassi, A., Hafidi, A., Khayet, M., García-Payo, Integrated direct contact membrane distillation for olive mill wastewater treatment, Desalination 323 (2013), 31-38, DOI: 10.1016/j.desal.2012.06.014.

Franken, A.C.M., Nolten, J.A.M., Bargeman, D., Mulder, M.H.V., Smolders, C.A., Influence of the structure of a microporous membrane on its wettability (Chapter 3), PhD thesis (1988), UTwente.

Gabelman, A., Hwang, S.T., Hollow fiber membrane contactors, Journal of Membrane Science 159 (1999), 61-106, DOI: 10.1016/S0376-7388(99)00040-X.

García-Payo, M.C., Izquierdo-Gil, M.A., Fernández-Pineda, C., Wetting Study of Hydrophobic Membranes via Liquid Entry Pressure Measurements with Aqueous Alcohol Solutions, Journal of Colloid and Interface Science 230 (2000), 420-431, DOI: 10.1006/jcis.2000.7106.

González-Muñoz, M.J., Luque, S., Álvarez, J.R., Coca, J., Recovery of phenol from aqueous solutions using hollow fibre contactors, Journal of Membrane Science 213 (2003), 181-193, DOI: 10.1016/S0376-7388(02)00526-4.

Hereijgers, J., Callewaert, M., Breugelmans, T., Ottevaere, H., Cabooter, D., De Malsche, W., A membrane microcontactor as a tool for integrated sample preparation, Journal of Separation Science 35 (2012), 2407-2413, DOI: 10.1002/jssc.201200477.

Hereijgers, J., Callewaert, M., Lin, X., Verelst, H., Breugelmans, T., Ottevaere, H., Desmet, G., De Malsche W., A high aspect ratio membrane reactor for liquid-liquid extraction, Journal of Membrane Science 436 (2013), 154-162, DOI: 10.1016/j.memsci.2013.02.020.

Jönsson J.A., Lövkvist, P., Audunsson, G., Nilvé, G., Mass transfer kinetics for analytical enrichment and sample preparation using supported liquid membranes in a flow system with stagnant acceptor liquid, Analytica Chimica Acta 277 (1993), 9-24, DOI: 10.1016/0003-2670(93)85084-W.

Kiani, A., Bhave, R.R., Sirkar, K.K., Solvent extraction with immobilized interfaces in a microporous hydrophobic membrane, Journal of Membrane Science, 20(1984), 125-145, DOI: 10.1016/S0376-7388(00)81328-9.

Kim, B.S., Harriott, P., Critical Entry Pressure for Liquids in Hydrophobic Membranes, Journal of Colloid and Interface Science 115 (1987), 1-8, DOI: 10.1016/0021-9797(87)90002-6.

Lawson, K.W., Lloyd, D.R., Membrane distillation, Journal of Membrane Science 124 (1997), 1-25, DOI: 10.1016/S0376-7388(96)00236-0.

Maruyama, T., Kaji, T., Ohkawa, T., Sotowa, K., Matsushita, H., Kubota, F., Kamiya, N., Kusakabe, K., Goto, M., Intermittent partition walls promote solvent extraction of metal ions in a microfluidic device, Analyst 129 (2004), 1008-1013, DOI: 10.1039/b411630p.

Mavroudi, M., Kaldis, S.P., Sakellaropoulos, G.P., A Study of mass transfer resistance in membrane gas-liquid contacting processes, Journal of Membrane Science 272 (2006), 103-115, DOI: 10.1016/j.memsci.2005.07.025.

North, R.C., Chemical Hazard Respons Information System, Cameo Chemicals, June 1999.

Pabby, A.K., Sastre, A.M., State-of-the-art review on hollow fiber contactor technology and membrane-based extraction processes, Journal of Membrane Science 430 (2013), 263-303, DOI: 10.1016/j.memsci.2012.11.060.

Pedersen-Bjergaard, S., Rasmussen, K.E., Electrokinetic migration across artificial liquid membranes: New concept for rapid sample preparation of biological fluids, Journal of Chromatography A 1109 (2006), 183-190, DOI: 10.1016/j.chroma.2006.01.025.

Prasad, R., Sirkar, K.K., Hollow fiber solvent extraction: performances and design, Journal of Membrane Science 50 (1990), 153-175, DOI: 10.1016/S0376-7388(00)80313-0.

Saffarini, R.B., Mansoor, B., Thomas, R., Arafat, H.A., Effect of temperature-dependent microstructure evolution on pore wetting in PTFE membranes under membrane distillation conditions, Journal of Membrane Science 429 (2013), 282-294, DOI: 10.1016/j.memsci.2012.11.049.

van Rijn, C.J.M., Membrane Sciences and Technology Series Volume 10: Nano and Micro Engineered Membrane Technology, Elsevier, The Netherlands, 2004, ISBN: 978-0-444-51489-9.

Wang, R., Zhang, H.Y., Feron P.H.M., Liang, D.T., Influence of membrane wetting on CO_2 capture in microporous hollow fiber membrane contactors, Separation and Purification Technology 46 (2005), 33-40, DOI: 10.1016/j.seppur.2005.04.007.

Zha, F.F., Fane, A.G., Fell, C.J.D., Schofield, R.W., Critical displacement pressure of a supported liquid membrane, Journal of Membrane Science 75 (1992), 69-80, DOI: 10.1016/0376-7388(92)80007-7.

Zolotarev, P.P., Ugrozov, V.V., Volkina, I.B., Nikulin, V.N., Treatment of waste water for removing heavy metals by membrane distillation, Journal of Hazardous Materials 37 (1994), 77-82, DOI: 10.1016/0304-3894(94)85035-6.